A comparison of two high performance inverse photoemission bandpass detectors

I. G. Hill and A. B. McLean
Department of Physics, Queen's University, Kingston, Ontario, K7L 3N6, Canada

(Received 24 July 1997; accepted for publication 17 September 1997)

By performing inverse photoemission experiments on the same sample at the same time with two different detectors, their performance has been directly compared. The first detector is based on one of the most promising solid-state detector designs. It is comprised of a focused mesh electron multiplier and a CaF_2 window. The second detector is a Geiger–Müller tube which uses dimethyl ether and a MgF_2 window. Although it has already been demonstrated that detectors based on this design work, the dimethyl ether Geiger–Müller tubes are not widely used, and we show that it is essential to compensate for detector dead time effects for the detector to be practicably useful. Once this is done, the dimethyl ether Geiger–Müller tube has a sensitivity that is approximately 20 times greater than that of the solid-state detector. Furthermore, it is easy to operate and it does not appear to suffer from the problems that are normally associated with iodine Geiger–Müller detectors. © *1998 American Institute of Physics.* [S0034-6748(98)02701-4]

I. INTRODUCTION

In inverse photoemission experiments[1–3] the most widely used bandpass detector is the iodine Geiger–Müller (GM) detector. Although, the iodine detector is conceptually simple, the problems associated with it are well documented.[4] For example, the sensitivity of the detector varies by as much as 8%/°C. Furthermore, iodine etches stainless steel and it is, by necessity, separated from the ultrahigh vacuum analysis chamber by only a thin alkali fluoride window.

Because of these drawbacks, considerable effort has been invested in exploring alternative detector designs. Two strategies have been pursued. The first has been to search for new gas/window combinations that equal or improve on the performance of the iodine detector without the drawbacks mentioned above. The second strategy has been to replace the GM tube with a solid-state detector. Photomultipliers,[5,6] channeltrons,[7] and channel electron multiplier plates[8] have all been used with various degrees of success. Although solid-state detectors are easy to operate, their quantum efficiency is considerably lower than that of GM tubes. Consequently, to improve the quantum efficiency, a variety of photoemissive coatings have been applied to the photocathodes and the photoemission thresholds of the coatings have been matched to the energy gap of the window material.[9]

One of the most promising solid-state detectors is the combination of a focused mesh electron multiplier and a CaF_2 window.[10–12] Because we were hesitant to use iodine GM tubes, for the reasons stated above, we originally built a solid-state detector based on this design. Although it was easy to operate, we were ultimately disappointed with the detector sensitivity. This led us to review the range of alternative gas/window combinations that had been explored in GM detectors. One of the most promising alternatives is the dimethyl ether/MgF_2 combination. Although proof of principle has already been demonstrated,[13] this detector has not been widely used. We built a detector, tested its performance and found that the dimethyl ether/MgF_2 combination is easy to use and very stable. However, in order to utilize this detector, attention has to be given to detector dead time effects. Since these are not always discussed,[13] and this may be the reason why this detector has not been more popular, we discuss them in detail here. Furthermore, we were in an ideal position to make a direct comparison between the solid-state and the dimethyl ether GM detectors. As they were both mounted in the same chamber, we could collect spectra concurrently from the same sample. This comparison illustrates the outstanding performance of the dimethyl ether/MgF_2 GM detector.

II. SOLID-STATE DETECTOR

The solid-state detector consisted of a focused mesh, 20 dynode, activated CuBe electron multiplier (Johnston Laboratories MM1). This detector is commonly used in inverse photoemission spectrometers.[10–12] The detector is used as a VUV photomultiplier, with the first dynode, either bare or coated with KCl to improve efficiency and resolution, acting as the photocathode. A photon energy bandpass can be realized by placing a CaF_2 window (2 mm thick, Bicron) in front of the photocathode. The combination of the quantum efficiency of the photocathode, which increases with increasing photon energy, and the transmission function of CaF_2, which cuts off sharply at the bulk band gap energy, forms a pass band of photon energies which are detected. The full width at half maximum of this band depends on the photocathode material, and is typically between 0.7 and 0.5 eV.[6]

Shielding and electrical isolation of the detector and its electrical connections were found to be the most important design criteria. The detector must be operated at very high voltages to achieve the gain necessary to detect single photoelectron pulses (typically 3.7–5 kV). Great care was therefore taken in mounting the detector and making electrical connections to avoid possible breakdown sites.

Shielding from both electrical noise and stray electrons was achieved by mounting the detector in an aluminum housing, which was completely sealed, except for a small

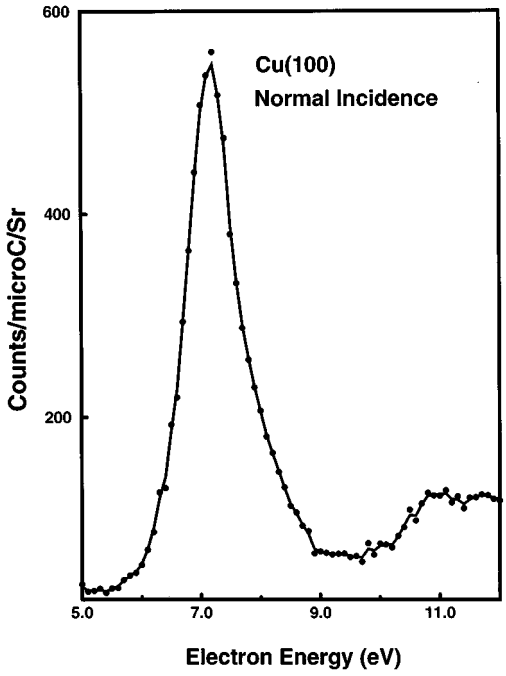

FIG. 1. The above figure shows an inverse photoemission spectrum from Cu (100) at normal incidence, collected using the MM1 detector. It can be directly compared with the data of Schäfer *et al.* (Ref. 11).

pump down hole. The hole was located as far as possible from the detector, and was connected to a series of baffle tubes on the interior of the housing, to further impede stray electrons. The CaF_2 window was sealed to the front of the detector housing using Viton O rings. This level of shielding may seem excessive, but it was found that merely blocking the line of sight was not sufficient. A leakage of a tiny fraction of the electrons used in an inverse photoemission experiment will create false counts many orders of magnitude larger than the true count rate.

Figure 1 is included to demonstrate the performance of our solid-state detector. The data was collected from Cu (100) at normal incidence, and can be directly compared to the spectrum presented by Schäfer *et al.*[11] The large peak is attributed to the unoccupied *p* states of Cu (100) near the Fermi level.[11] The maximum count rate that we observed on this peak is a factor of 3 lower than that reported by Schäfer *et al.* Their detector differs from ours in their use of a KBr photocathode, compared to a KCl, which may explain the discrepancy. The count rates may also be affected by differences in the transparency of the CaF_2 windows, errors in the estimates of the solid angles, or physical differences in the individual MM1 multipliers.

III. GEIGER–MÜLLER DETECTOR

The dimethyl ether GM tube consisted of a 2.5 cm diameter, 17.5 cm long stainless steel tube, a MgF_2 window, and a center electrode. The center electrode was a 1.5 mm diameter stainless steel wire, which was supported at one end by two PTFE spacers. The MgF_2 window (2 mm thick, Bicron) was sealed to the end of the tube using UHV epoxy (Varian, TorrSeal).

Although the detector was based on a previous design,[13] several important modifications were made. The detector as built was found to suffer from a severe quenching problem. This is caused by energetic positive ions, when reaching the walls of the tube following a detection event, having a finite probability of liberating an electron from the tube wall, which causes another avalanche and a false count to be detected.[14,15] Obviously, if this problem is too severe, it will cause the tube to be completely unstable with a single detection event leading to a continuous series of avalanches. If the probability is not too high, it may only lead to the washing out of an inverse photoemission spectrum, due to the slow reaction of the tube to a variation in the photon flux. This was found to be the case with our detector.

The problem of quenching is commonly encountered in nuclear detection techniques.[14] A quench gas is usually added to a GM tube to stabilize its response. Typically an organic gas, such as ethanol, is added. Energetic ions tend to collide with the quench gas, which absorbs much of the kinetic energy by dissociation of the complex molecules. The remnants of the organic molecule have a much lower probability of liberating an electron at the tube wall, effectively quenching the avalanche.

Following this idea, the gas mixture used in the detector was modified by the addition of a moderate partial pressure of ethanol. The final gas mixture used was: $\approx$380 mTorr dimethyl ether, $\approx$1.15 Torr ethanol, and $\approx$100 Torr argon. The dimethyl ether serves as the detection gas, being photoionized by the vuv photons. The argon acts as the multiplier gas, providing the electrons for the GM avalanche. The ethanol acts as a quench gas, to control the avalanche after the completion of a detected event. All pressures were measured using a Convectron gauge. The dimethyl ether and ethanol partial pressures are uncorrected, and the argon pressure was calculated using correction factors supplied by the gauge manufacturer.

With the exception of the original papers in this field,[1] very few inverse photoemission studies address the problem of detector dead time. GM tube dead time, or the time after a single event that the tube is incapable of detecting a second event, is typically several hundred microseconds.[14,15] This dead time is simply related to the time required for the positive ions created in a GM avalanche to drift to the tube walls, and restore the electric field at the center electrode. Assuming Poisson photon statistics, counting losses on the order of 10% can occur for count rates of several hundred counts s^{-1}, which is easily achievable. Furthermore, since the percentage of lost counts increases with increasing count rate, the net effect is to flatten spectral peaks and therefore decrease resolution. Although dead time correction formulae can be derived for various dead time models,[14] they only apply in the limit of large numbers, which is seldom realized in inverse photoemission.

To improve the performance of the detector, a dead time gating system was designed. The photon count rate was measured using a standard counter/timer unit. The timer was typically set to 1 s, and the unit counted the number of events within that period. The gating electronics disabled the counter/timer for a length of time greater than the dead time

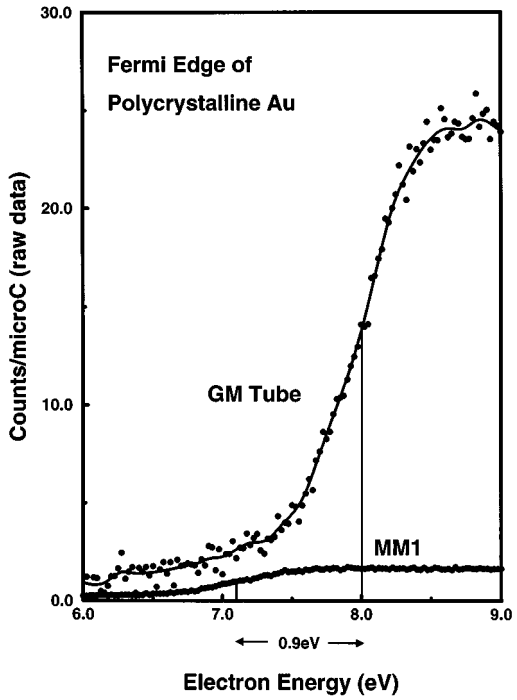

FIG. 2. This figure shows a direct comparison of count rates, and photon energy sensitivities between the MM1 and dimethyl ether GM tube detectors. The spectra were collected consecutively from the same evaporated polycrystalline Au sample. The bottom spectrum is the raw MM1 data. The top spectrum is the raw data from the GM tube. The solid lines are smoothed fits to the data. The energy difference between the midpoints of the Fermi step is 0.9 eV, which is indicated in the figure. This agrees with the nominal photon energies of the MM1 and GM tube which are 9.7 eV and 10.6 eV, respectively.

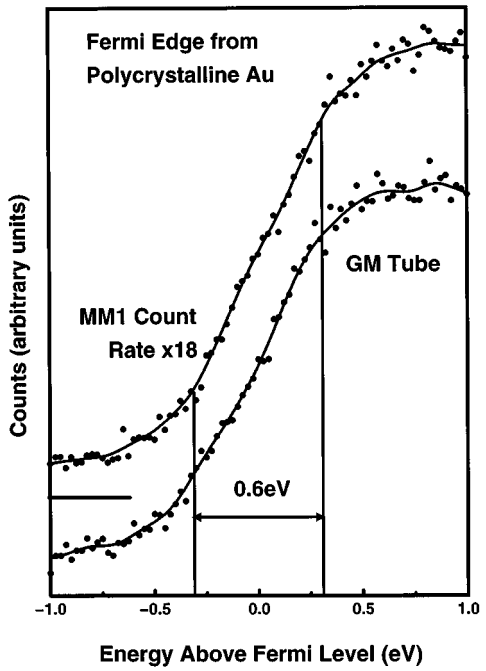

FIG. 3. This figure contains the same spectra as presented in Fig. 2, with the MM1 data multiplied by 18, and shifted vertically. The energy scales of each spectrum have been shifted to align their Fermi levels. The resolution of each detector was estimated to be approximately 0.6 eV. The collection time of the MM1 data was 20 times that of the GM data.

after each count. The electronics also disabled the electron source for the same length of time, therefore making a second detector event impossible until the tube has completely recovered. The counter/timer counts the number of events which occur within a period of detector live time equal to the timer setting. The total charge incident on the sample during this time is measured by a charge integrating amplifier which is discharged by the gating electronics after every timer cycle (each second).

IV. PERFORMANCE COMPARISON

Both inverse photoemission detectors were mounted with their axes at angles of 45° to the sample normal. The detector entrance windows were of equal diameter, and were equidistant from the sample, such that the solid angles subtended, ≈ 0.04 Sr, were equal. The direct comparison of observed count rates is therefore valid. All MM1 spectra shown were collected with a 1000 Å KCl photocathode evaporated onto the first dynode, which increased the detector sensitivity by a factor of ≈ 3.5 compared to the bare dynode.

Figure 2 shows inverse photoemission spectra of freshly evaporated polycrystalline Au, collected from both detectors. The two spectra shown are the raw data from the MM1 detector and the GM tube. It is obvious that the GM tube has much greater sensitivity than the MM1 detector. The increased count rate is of great importance in inverse photoemission of reactive surfaces, or surfaces with surface states

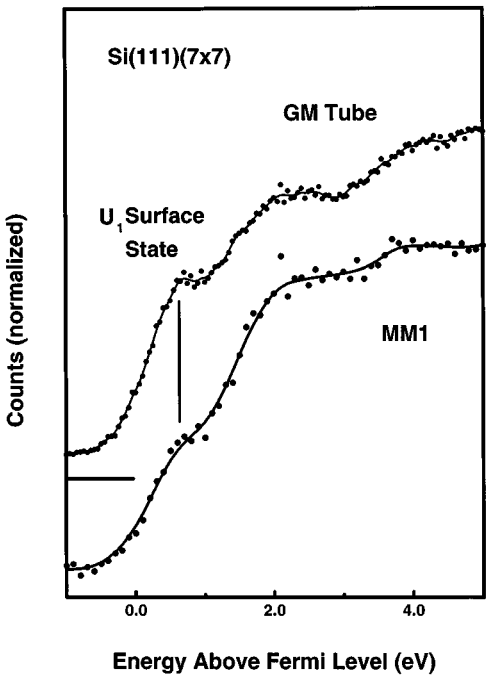

FIG. 4. Inverse photoemission spectra of Si (111) (7×7) from the GM tube (top), and the MM1 detector (bottom). The MM1 data has been smoothed by convolution with a Gaussian width of 0.300 eV full width at half maximum, while the GM spectrum presented is raw data. Notice the improved sharpness of the surface state, U_1, in the GM tube spectrum. The state in the MM1 spectrum is washed out by the smoothing process. Each spectrum has been shifted by the difference between its detector's mean photon energy and the electron gun cathode work function, to give the spectral energy relative the Fermi level.

with low cross sections, where the reactivity of the surface limits the number of spectra which can be collected in a single run.

The difference between the nominal photon energies of the two detectors can be estimated from the difference between the incident electron energies at the midpoints of each Fermi level onset. The photon energy is equal to the sum of the incident electron energy at this point and the work function of the electron gun cathode. The increased photon energy of the GM tube allows the electron gun to be operated at higher energies, where the beam characteristics are generally better.

Figure 3 contains the same spectra as Fig. 2, with the MM1 data multiplied by 18, and the energy scales shifted to align the Fermi levels of each. The Fermi level spectra look very similar, and the resolution of each detector was estimated to be 0.6 eV. No smoothing has been applied to either spectrum. To achieve comparable counting statistics, the MM1 was allowed to collect data for 20 times as long as the GM tube.

Figure 4 is another direct comparison of the capabilities of the two detectors. The figure contains normal incidence inverse photoemission spectra of Si (111) (7×7). The GM data is raw, while the MM1 data has been smoothed by convolution with a Gaussian width of 0.300 eV full width at half maximum. The smoothing was necessary to compensate for the inferior counting statistics, and has the unfortunate consequence of lowering the ''effective'' resolution. These spectra were not taken at the same time nor from the same sample, but the better effective resolution of the GM tube is evident in the shape of the unoccupied surface state, U_1, located at ≈0.6 eV above the Fermi level. Again, it must be remembered that the GM tube can achieve equivalent counting statistics in $\approx1/20$th the time.

ACKNOWLEDGMENT

The authors would like to thank the Natural Sciences and Engineering Research Council of Canada for financial support.

[1] V. Dose, Prog. Surf. Sci. **13**, 225 (1983).
[2] N. Smith, Rep. Prog. Phys. **51**, 1227 (1988).
[3] F. Himpsel, Surf. Sci. Rep. **12**, 1 (1990).
[4] G. Denninger, V. Dose, and H. Scheidt, Appl. Phys. **18**, 375 (1979).
[5] N. Sanada, M. Shimomura, and Y. Fukuda, Rev. Sci. Instrum. **64**, 3480 (1993).
[6] K. Yokoyama *et al.*, Rev. Sci. Instrum. **64**, 87 (1993).
[7] R. Avci, Q. Cai, and G. Lapeyre, Rev. Sci. Instrum. **60**, 3643 (1989).
[8] W. Sheils, R. Leckey, and J. Riley, Rev. Sci. Instrum. **64**, 1194 (1993).
[9] F. Schedin, G. Thorton, and R. Uhrberg, Rev. Sci. Instrum. **68**, 41 (1997).
[10] N. Babbe *et al.*, J. Phys. E **18**, 149 (1985).
[11] I. Schäfer *et al.*, Rev. Sci. Instrum. **58**, 710 (1987).
[12] H. Carstensen, R. Claessen, R. Manzke, and M. Skibowski, Phys. Rev. B **41**, 9880 (1990).
[13] K. Prince, Rev. Sci. Instrum. **59**, 741 (1988).
[14] G. F. Knoll, *Radiation Detection and Measurement*, 2nd ed. (Wiley, New York, 1989).
[15] J. A. R. Samson, *Techniques of Vacuum Ultraviolet Spectroscopy* (Wiley, New York, 1967).